Available online at www.sciencedirect.com
ScienceDirect
Journal of the European Ceramic Society 28 (2008) 2199–2211
www.elsevier.com/locate/jeurceramsoc

Thermal stability of zircon ($ZrSiO_4$)

Arno Kaiser, Markus Lobert, Rainer Telle *

Institut fuer Gesteinshuettenkunde (Department of Mineral Engineering), RWTH Aachen University, Mauerstrasse 5, 52064 Aachen, Germany

Received 4 September 2005; received in revised form 27 November 2007; accepted 9 December 2007
Available online 23 April 2008

Dedicated to Professor Dr. Eduard Woermann, RWTH Aachen University, Chair of Technical Mineralogy, born 24th November 1929, died 28th March 2008, to memorise his achievements in phase diagrams of industrial mineral systems

Abstract

Based on annealing experiments with natural and synthetic raw materials of known grain size and impurity level as well as single crystals the temperature of thermal dissociation of $ZrSiO_4$ was assessed at $1673 \pm 10\,^{\circ}C$. $ZrSiO_4$ decomposes by a solid-state reaction releasing SiO_2 in form of discrete metastable intermediate phases with superstoichiometric Si-content. The eutectic temperature in the ZrO_2–SiO_2 system was set to $1687 \pm 10\,^{\circ}C$. The thermodynamic dataset for the ZrO_2–SiO_2 system was optimised and the quasi-binary phase diagram was re-calculated. The significant influence of even small amounts of impurities on the decomposition temperature and kinetics is explained by the formation of low melting liquid phases resulting in the favoured dissolution of solid silica immediately after release from the zircon structure.

Keywords: Phase diagram; $ZrSiO_4$; ZrO_2; SiO_2; Structure; Microstructure; Powders; Solid-state reaction

1. Introduction

The interest in zircon ($ZrSiO_4$) as a ceramic and refractory material is due to its excellent thermo-physical properties such as low thermal expansion, low thermal conductivity, as well as a good corrosion resistance, for example, against glass melts, slag and liquid metal alloys.[1,2] Accordingly, zircon has a wide range of application as a construction material in glass tanks, in iron and steel production, in energy technology, as moulds and cores in precision investment casting or as protective coatings of steel-moulding tools.

In spite of the fact that all these high-temperature applications strongly depend on the accurate knowledge of the thermal stability of $ZrSiO_4$ available information about this topic differs enormously concerning both dissociation mechanism and temperature. Although most publications agree that zircon decomposes by a solid-state reaction the stated dissociation temperatures vary between 1285 and 1700 °C, resulting in different phase diagrams published. These data are, however, most important for prediction of life-time of zircon and zirconia-based refractory bricks and parts in contact with silica-containing melts. Moreover, investment casting of high-temperature alloys such as nickel-based super alloys or titanium aluminides requires temperatures exceeding 1600 °C which is close to the decomposition temperature of zircon. Since knowledge of the pseudo-binary oxide system ZrO_2–SiO_2 is a prerequisite for the understanding of higher order systems most care should be taken regarding experiments, purity, particle size, and microstructural analysis.

The aim of this work is to review and to assess both thermodynamic and kinetic background on the reaction $ZrSiO_4 \leftrightarrow ZrO_2 + SiO_2$ taking the presence of small amounts of impurities into account which are considered to influence the reaction significantly. As a consequence, zircon single crystals as well as natural raw materials were used in the present work for the exact determination of the dissociation temperature and mechanism.

2. Literature review of the quasi-binary phase system

Table 1 gives an overview on the thermal stability of zircon as published earlier. The strong variations[3] may be generally explained by the fact that the decomposition reaction takes place at a temperature close to the eutectic melt formation and may therefore been not recognized upon heating too fast.[4]

* Corresponding author. Tel.: +49 241 809 4968; fax: +49 241 809 2226.
E-mail address: telle@ghi.rwth-aachen.de (R. Telle).

0955-2219/$ – see front matter © 2008 Elsevier Ltd. All rights reserved.
doi:10.1016/j.jeurceramsoc.2007.12.040

Table 1
Statements on the high-temperature dissociation of zircon

Authors	Year	Mechanism	Temperature (°C)
Washburn and Libman	1920	Congruent melting	2550
Zhirnowa	1934	Congruent melting	2430
Geller and Lang	1945	Incongruent melting	1775
Curtis and Sowman	1953	Solid-state dissociation	1540
Toropov and Galakhov	1956	Solid-state dissociation	1540
Cocco and Schromek	1958	Incongruent melting	1720
Butterman and Foster	1967	Solid-state dissociation	1676
Anseau, Biloque, Fierens	1976	Solid-state dissociation	>1525–1634
Klute and Woermann	1982	Solid-state dissociation	1681 ± 5
Kanno	1989	Solid-state dissociation	1650–1700
Kocyan and Meulenberg	1997	Solid-state dissociation	>1550
Levin	2001	Solid-state dissociation	1550
Pavlik and Holland	2001	Solid-state dissociation	1285
O'Neill	2003	Solid-state dissociation	1667

Curtis and Sowman carried out one of the most detailed studies in 1953.[5] Zircon samples were annealed between 1400 and 2000 °C for 2 h followed by cooling down for 45 min. The influence of annealing time and cooling rate was considered as well. The decomposition reaction starts at 1556 °C and accelerates with increasing temperature. Quenching after annealing resulted in higher zirconia content since the reverse reaction was suppressed in this way. All experiments revealed, however, residual monoclinic zirconia and a glassy phase. Samples were also heated far above the decomposition temperature, quenched and re-annealed for 8 h at various temperatures. Zircon already decomposed re-associated between 1278 and 1556 °C with a maximum reaction rate above 1444 °C. Zircon formation starting from ZrO_2 and quartz, cristobalite, tridymite or amorphous silica did not show any significant dependence on the starting silica modifications. The lowest formation temperature observed was 1333 °C which is only a little higher than the lowest temperature of re-association, i.e. 1278 °C. Consequently, Curtis and Sowman considered a solid-state reaction for the decomposition and corrected the earlier phase diagrams accordingly (Fig. 1).

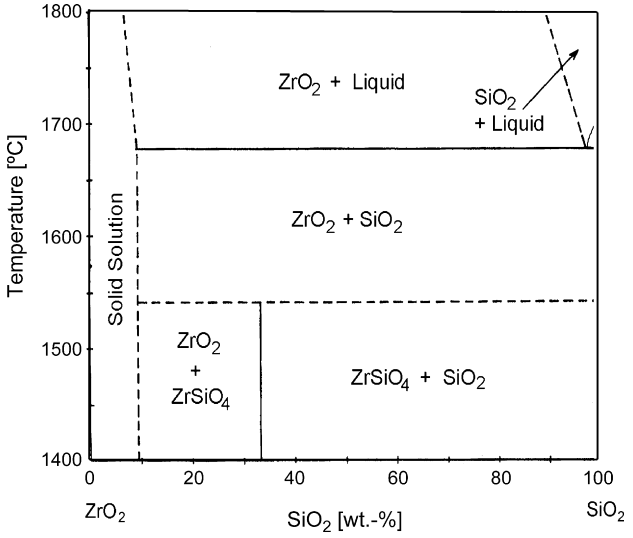

Fig. 1. ZrO_2–SiO_2 phase diagram after Curtis and Sowmann.[5]

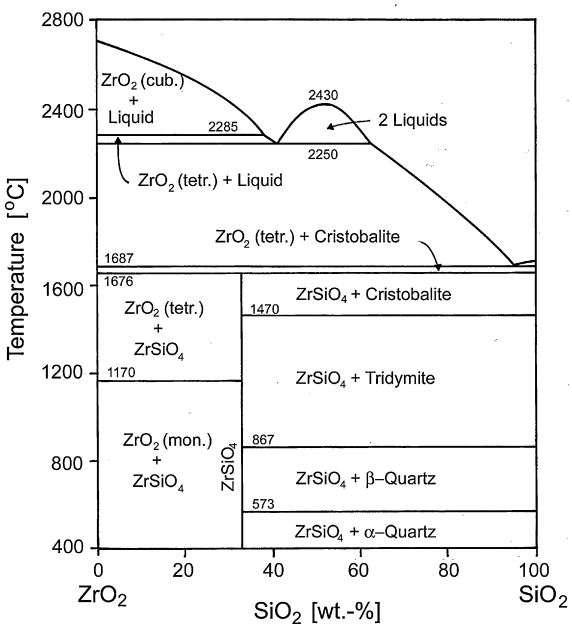

Fig. 2. ZrO_2–SiO_2 phase diagram, after Butterman and Foster.[4]

Butterman and Foster determined both the maximum formation temperature of zircon from the mixed oxides. The minimum decomposition temperature of zircon was found to be 1676 ± 7 °C, yielding the phase diagram shown in Fig. 2.[4] The existence of two immiscible liquids was taken unproved from Toropov et al.[6] It should be pointed out that the raw materials of Toropov et al. contained a considerable amount of yttria compounds and apatite from natural mineral intergrowths.

McPherson et al. used plasma-dissociated zircon (PDZ) as a model mixture of both oxides to study the reaction since ZrO_2 formed spherolithic particles of the monoclinic modification in a SiO_2 matrix after quenching.[7] The formation of zircon started slowly at 1500 °C. Increasing the specific surface area by intensive milling yielded a strong acceleration of the reaction, which was explained by an improved heterogeneous nucleation at the fracture surfaces. This result indicated that the entire process is nucleation controlled but not diffusion controlled. Fast quenched PDZ of the tetragonal modification and a particle size below 20 nm resulted in an onset of zircon formation at 1200 °C while the reaction was completed at 1450 °C.

Mori et al.[8] continued to study the influence of heterogeneous nucleation. They stated that a significant amount of nucleation is limited to the temperature range only between 1200 and 1300 °C. Starting from sol–gel-derived oxide mixtures, zircon formation was observed at 1200 °C only after 13 h annealing time.

Kanno[9] paid attention to thermodynamic and crystallographic viewpoints of the reaction. The decomposition of zircon powders was established at 1600–1700 °C. Ground and sol–gel-derived ZrO_2–SiO_2 powder blends showed zircon formation at 1500 °C whereas more zircon was formed using ground material.

Tartaj et al.[10] started from amorphous ZrO_2–SiO_2 powder blends and observed the crystallisation of zircon at 1350 °C, traces of cristobalite were found above 1450 °C by high-temperature X-ray measurements. The reaction rate increased up to 1550 °C and dropped again at above 1600 °C. The fact

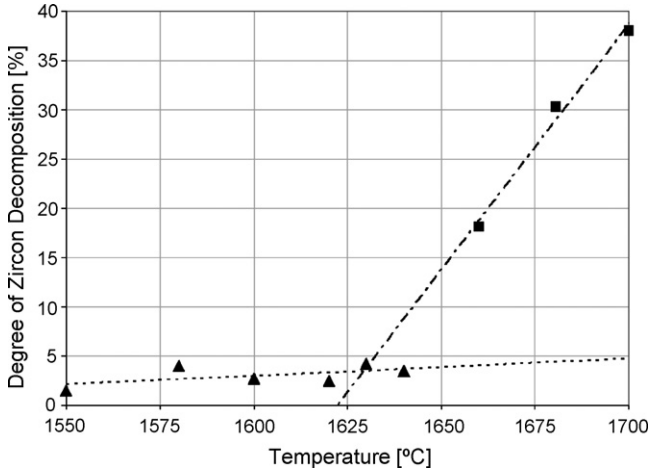

Fig. 3. Degree of zircon decomposition vs. temperature, drawn according to data by Anseau et al.[11]

that the dissociation temperature had not been reached yet was explained by a decrease in driving force.

Anseau et al. studied the thermal decomposition of natural Australian zircon sand.[11] The purity was given as 99.13%, the major impurities being 0.32 wt.% Al_2O_3, 0.25 wt.% TiO_2, and 0.15 wt.% Fe_2O_3. They measured the degree of decomposition by chemical analysis of the amount of free SiO_2 as well as by the $ZrO_2/ZrSiO_4$ ratio as recorded by XRD. The samples were heated at 300 K/min to temperatures between 1400 and 1690 °C and kept for 8 h. Fig. 3 shows the degree of dissociation as a function of temperature. The decomposition starts obviously in the solid state between 1525 and 1550 °C at a relatively low velocity. At 1650 °C, approximately, the reaction accelerates significantly.

Klute[12] synthesised high-purity zircon powder according to the petroleum drying method developed by Reijnen et al.[13] The starting chemicals ethyl silicate and zirconyl sulfate were mixed as an aqueous solution dispersed at a molecular level and were dehydrated by a hot petroleum bath. After sedimentation the precipitates were extracted and thermally decomposed at 1050 °C yielding a molecular mixture of oxides. These powders were wrapped into a platinum foil and heated in a calibrated furnace for 1–2 days in air at several temperatures. After air quenching to room temperature the samples were characterised by XRD. Kinetic evaluation was carried out by plotting the peak intensity ratio of the (1 1 $\bar{1}$)-reflection of baddeleyite and of the (1 0 1)-reflection of zircon versus the annealing temperature (Fig. 4). The thermodynamic point of decomposition is obtained by the intersection of the extrapolated curves at 1681 ± 5 °C. This result is in good agreement with that of Butterman and Foster, which was 1677 °C.[4] The binary eutectic between ZrO_2 and SiO_2 taken as the disappearance of cristobalite in the XRD spectrum, was set by Klute at 1699 ± 3 °C, which is also in good agreement with 1687 °C as reported by Butterman and Foster.[4]

Pavlik et al.[14] studied the dissociation of both 98% pure and purified $ZrSiO_4$. Impure particles of <45 μm in size decomposed after 8 h at 1285 °C. The authors suggested that smaller particles should dissociate at even lower temperatures. In contrast, pure particles still showed 50% residual $ZrSiO_4$ after 7 h at 1650 °C.

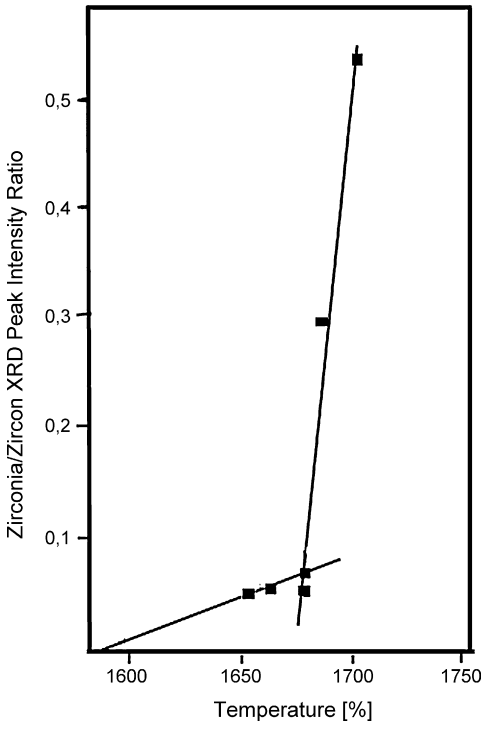

Fig. 4. Degree of zircon decomposition as measured by the XRD peak intensity ratio of $ZrO_2/ZrSiO_4$, re-drawn from Klute et al.[12]

3. Experimental

Since there is evidence that both particle size and impurities, even if present as traces, may influence nucleation and the type of mass transport mechanism during dissociation and formation of zircon, experiments were carried out using different particle sizes and levels of natural impurities. In addition, single crystal studies were undertaken to exclude these influences as far as possible.

3.1. Raw materials and processing

For the study of the zircon decomposition reaction and temperature natural raw materials (powders A–G in Table 2) of different grain size and purity have been used. The purities and main impurity phases of the different powders used in this work are listed in Table 2. The specific surface areas (BET) and grain sizes d_{10}, d_{50} and d_{90} are summarized in Fig. 5. The dependence of the zircon decomposition on particle size has been studied with powders of identical purity grade but different grain size and specific surface area (powders A + C and powders B + D + F + G).

Starting powders (powders H–M in Table 2) for the examination of the formation reaction of zircon from the oxide compounds were a yttria-stabilised zirconium oxide (TZ-3Y of Tosoh Ltd., Tokyo, Japan) and an unstabilised monoclinic zirconium oxide (Fumed Zirconium Dioxide ZR-ET, Degussa, Germany) in combination with fumed and fused silica as well as cristobalite of different grain size. Additionally a thermally decomposed zircon powder (Cerdec GmbH, Frankfurt, Germany) was tested.

Table 2
Purity and impurities of powders used as raw materials

Powder		Supplier	Purity (supplier analysis)		Phase composition (XRD)
			wt.%	Impurities	
A	$ZrSiO_4$ < 1 μm LOT G07H01	Alfa Aesar, GmbH & Co KG	100		$ZrSiO_4$
B	$ZrSiO_4$ < 3 μm microfine	RZM Pty., Europe	>98.3	Al_2O_3, TiO_2, Fe_2O_3, P_2O_5	$ZrSiO_4$
C	$ZrSiO_4$ < 4 μm LOT I15I23	Alfa Aesar, GmbH & Co KG	100		$ZrSiO_4$
D	$ZrSiO_4$ < 9 μm standard fine	RZM Pty., Europe	>98.3	Al_2O_3, TiO_2, Fe_2O_3, P_2O_5	$ZrSiO_4$
E	$ZrSiO_4$ < 90 μm calcined	Mineralmühle Leun, Rau GmbH (mined at Starke, Florida; DuPont, USA)	>97.9	Al_2O_3, TiO_2, Fe_2O_3, P_2O_5	$ZrSiO_4$
F	$ZrSiO_4$ < 56 μm Zirconflour Din 100	RZM Pty., Europe	>98.3	Al_2O_3, TiO_2, Fe_2O_3, P_2O_5	$ZrSiO_4$
G	$ZrSiO_4$ < 90 μm, Zirconflour Din 70	RZM Pty., Europe	>98.3	Al_2O_3, TiO_2, Fe_2O_3, P_2O_5	$ZrSiO_4$
H	Aerosil 200 + ZrO_2 (TZ-3Y/Lot Z307441P)	Degussa AG, Tosoh Corporation	>99.8, >99.0	Al_2O_3, TiO_2, Fe_2O_3; Al_2O_3, Fe_2O_3, Na_2O, SiO_2	SiO_2 (amorph.), ZrO_2 (tetrag.)
I	Fused silica + ZrO_2 (TZ-3Y/Lot Z307441P)	Quarzwerke GmbH, Tosoh Corporation	>99.7, >99.0	Al_2O_3, Fe_2O_3, Na_2O, SiO_2; Al_2O_3, Fe_2O_3, Na_2O, K_2O	SiO_2 (amorph.), ZrO_2 (tetrag.)
J	Sikron Feinstmehl Cristobalit SF600 + ZrO_2 (TZ-3Y/Lot Z307441P)	Quarzwerke GmbH, Tosoh Corporation	>99.0, >99.0	Al_2O_3, Fe_2O_3, Na_2O, K_2O, CaO, MgO; Al_2O_3, Fe_2O_3, Na_2O, SiO_2	Cristobalite, ZrO_2 (tetrag.)
K	Silmikron Ultrafeinstmehl Cristobalit (Vp 805-10/1) + ZrO_2 (TZ-3Y/Lot Z307441P)	Quarzwerke GmbH, Tosoh Corporation	>98.5, >99.0	Al_2O_3, Fe_2O_3, Na_2O, K_2O, CaO, MgO; Al_2O_3, Fe_2O_3, Na_2O, SiO_2	Cristobalite, ZrO_2 (tetrag.)
L	Thermally decomposed zircon	Cerdec GmbH	>99.0	Al_2O_3, Fe_2O_3	SiO_2 (amorph.), ZrO_2 (monocl.)
M	Aerosil 200 + fumed zirconium dioxide ZR-ET (unstabilised)	Degussa AG	>99.8, >97.0	Al_2O_3, TiO_2, HCl, Fe_2O_3; HfO_2 2%, Al_2O_3, Fe_2O_3, free SiO_2	SiO_2 (amorph.), ZrO_2 (monocl.)

In order to prepare ZrO_2/SiO_2-blends the powders were mixed stoichiometrically for 48 h in water or alcohol on a roller bank. Green bodies were prepared by uniaxial pre-pressing to cylindrical bodies of 15 mm diameter and 5 mm height and finally cold isostatically pressing at 50–400 kN.

3.2. Thermal treatment

Thermal treatment was carried out by several methods. High-temperature X-ray analysis was employed first to obtain information on phase changes, at heating rates of 3 K/min recording the phase composition at steps of 50 K from 1100 °C upwards. Thermally decomposed zircon powder was analysed at heating rates of 1 K/min gathering X-ray spectra every 10 K above 1200 °C. All high-temperature X-ray diffraction experiments were performed in air using a Siemens Kristalloflex D500 diffractometer with Cu Kα radiation (40 kV, 30 mA) and a Rigaku high-temperature chamber.

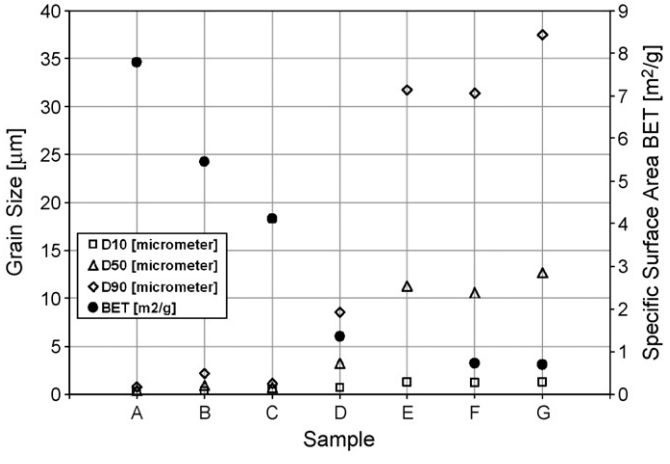

Fig. 5. Grain size and specific surface area of the used natural zircon raw materials.

The powder compacts were also sintered between 1000 and 1700 °C with a heating rate of 3 K/min and holding time between 1 and 6 h. Cooling rates were 5 and 30 K/min.

After thermal treatment sintered samples were characterised by X-ray diffraction at room temperature using a Philips PW 3020-goniometer with PW 3710-controller and Cu Kα radiation at 40 kV and 40 mA, by scanning electron microscopy (LEO REM 440i) and by transmission electron microscopy (FEI Tecnai F20), both combined with EDS-analysis.

3.3. Single crystal experiments

To separate the effect of grain size, grain size distribution and intergrown impurities of the natural zircon powders single crystal experiments were carried out. For this purpose a natural uncoloured and, within the range of chemical resolution, pure zircon single crystal from Cambodia was oriented by single crystal X-ray diffraction and then cut into slices parallel to the tetragonal *c*-axis. Along the crystallographic *c*-axis the $ZrSiO_4$-structure exhibits chains of alternating SiO_4-tetrahedra and ZrO_8-coordination polyhedra, the observation of which could provide information on the dependence of the $ZrSiO_4$-

Table 3
Decomposition temperatures of $ZrSiO_4$, heating rate 3 K/min (HT-XRD) and 20 K/min up to 1000/1200 °C and 5 K/min to sintering temperature (sintering)

Sample	Sample	Purity (%)	Start of decomposition (formation of zirconia)	
			HT-XRD (up to 1550 °C)	Sintering
A	$ZrSiO_4$ < 1 μm	100	No decomposition at 1550 °C	1600 °C/4 h
B	$ZrSiO_4$ < 3 μm	>98.3	1450 °C	1500 °C/4 h
C	$ZrSiO_4$ < 4 μm	100	No decomposition at 1550 °C	1650 °C/2 h
D	$ZrSiO_4$ < 9 μm	>98.3	1450 °C	1500 °C/4 h
E	$ZrSiO_4$ < 90 μm	>97.9	No decomposition at 1450 °C	1550 °C/5 h
F	$ZrSiO_4$ < 56 μm	>98.3	1500 °C	1550 °C/4 h
G	$ZrSiO_4$ < 90 μm	>98.3	1500 °C	1550 °C/4 h

decompositon on specific crystallographic orientations. After cleaning with acetone, these slices were wrapped in a platinum foil and placed on an alumina carrier. Annealing was carried out at 1650, 1660, 1670, 1680, 1690 and 1700 °C with holding times of up to 16 h. With the exception of the 1650 °C sample, which was quenched in water, all other samples with higher annealing temperatures were cooled in the furnace at the maximum cooling rate available.

4. Experimental results

4.1. Annealing of powder-based samples

High-temperature X-ray experiments (Table 3) below 1600 °C did not show any indication of zircon decomposition under the given conditions when "100%" pure material (powders A and C) was used. Samples made of 98% pure $ZrSiO_4$ (powders B, D, F, and G) showed tetragonal ZrO_2 as a decomposition product from 1450 °C upwards depending on grain size, starting from 1450 °C for powder B with the finest grain size up to 1500 °C for the coarse grained powders F and G. During heat treatment of powders with 98% purity at 1400 °C, even after 10 h annealing, neither ZrO_2 nor SiO_2 were detected.

At higher temperature there is a much clearer evidence for the dependence of the zircon decomposition rate from grain size as shown in Fig. 6 for powders B, D, G with identical impurity grade. With decreasing grain size and increasing specific surface area, respectively, an accelerated dissociation kinetics of zircon is observed. Additionally the diagram shows for 1650 and 1700 °C samples, the strong temperature dependence of the zircon decomposition.

At 1600 °C compacts with small grain size <1 and <4 μm with highest purity revealed tetragonal ZrO_2 and amorphous SiO_2. At 1600 °C the decomposition of $ZrSiO_4$ starts without delay (Table 3).

Samples of stoichiometric blends of ZrO_2/SiO_2 powders revealed an instantaneous formation of $ZrSiO_4$ at 1230 °C during continuous heating. If annealed at 1200 °C formation of $ZrSiO_4$ was observed only after 4 h. After 230 min at 1300 °C, the reaction was considered completed since only zircon could be detected. This was also found at 1450 °C. In all cases the newly formed zircon decomposed again at temperatures above 1500 °C into tetragonal ZrO_2 and amorphous SiO_2. Fig. 7 shows the result of a high-temperature X-ray diffraction experiment for a fumed silica–tetragonal zirconia powder mixture (powder H) showing the rapid formation of $ZrSiO_4$ above 1300 °C and its decomposition starting at about 1480 °C. All blends containing yttria-stabilised zirconia behaved in the same way independently of the grain size and the silica structure (fused and fumed silica, as well as cristobalite of different grain size).

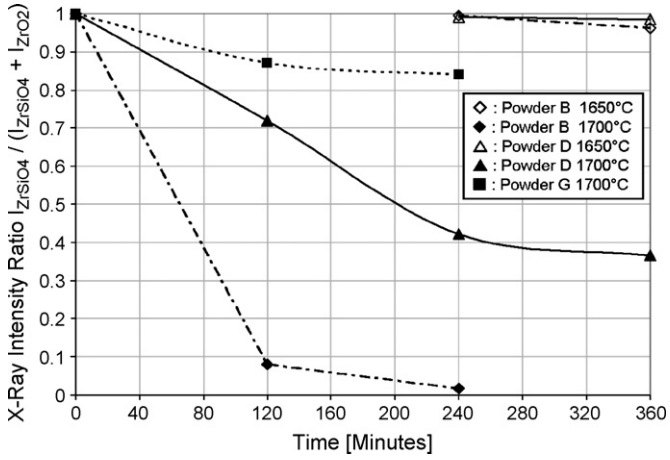

Fig. 6. Dissociation kinetics of zircon at 1650 and 1700 °C.

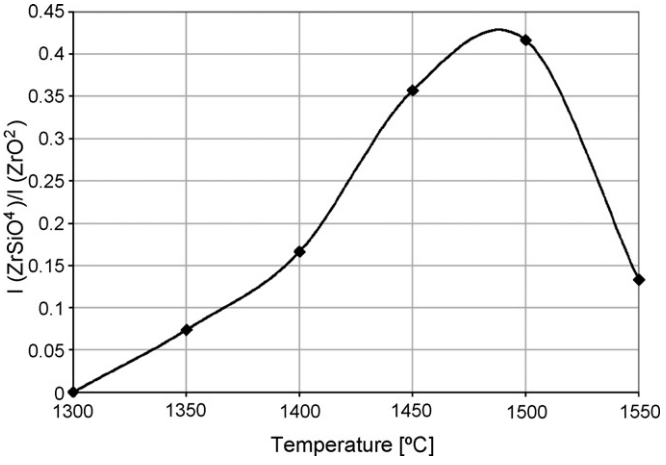

Fig. 7. Formation of $ZrSiO_4$ from a fumed silica–tetragonal zirconia powder mixture as a function of temperature.

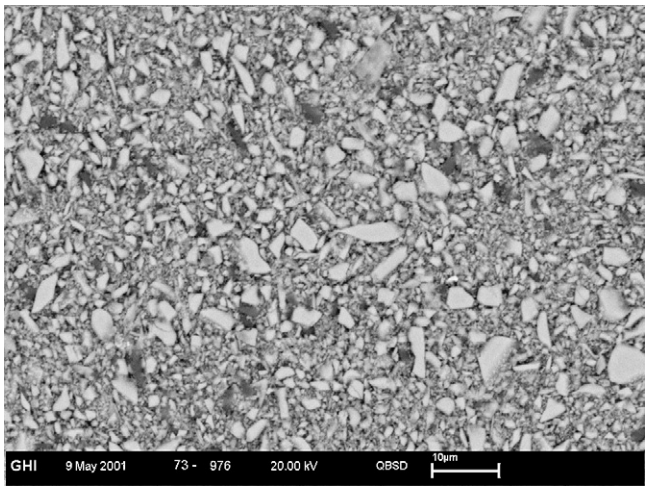

Fig. 8. $ZrSiO_4 < 1\ \mu m$, 4 h anneal at 1200 °C, light grey: $ZrSiO_4$, grey matrix: SiO_2. Scale = 10 μm.

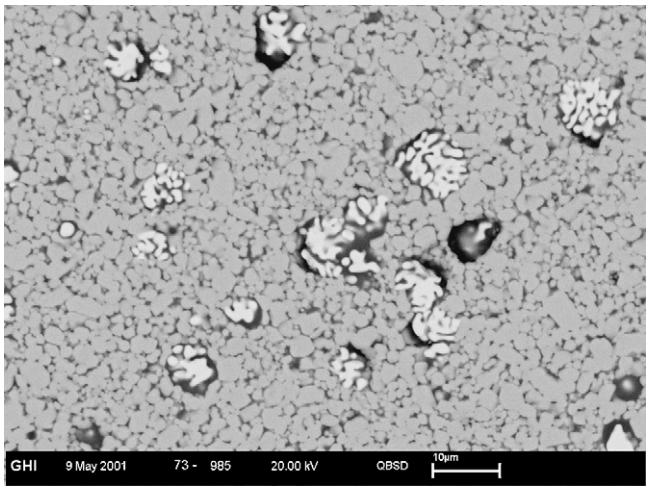

Fig. 10. $ZrSiO_4 < 1\ \mu m$, 2 h anneal at 1700 °C, black: glassy phase and pores, white: ZrO_2, grey: residual $ZrSiO_4$. Scale = 10 μm.

4.2. Sintering of powder-based $ZrSiO_4$ samples

Microstructural analysis of sintered samples prepared from high-purity powder A (original grain size <1 μm) shows a progressive densification of the zircon grains (Figs. 8 and 9). After 4 h annealing at 1550 °C, 98% pure material (powders B, D, F, G, with different grain sizes) exhibits a liquid phase and ZrO_2 particles at the grain boundaries of the original zircon crystals. At 1600 °C, a liquid phase is also formed in 100% pure material. After 2 h at 1700 °C, in both cases the zirconia particles grow to isolated clusters of rounded dendrites of 10 μm with amorphous silica in-between (Fig. 10), but with a much higher degree in the 98% pure material.

Sintering of large-grained zircon of lowest purity grade (<98%), e.g. Leun material (powder E), showed similar features, but with much clearer microstructural details. After 5 h at 1500 °C the microstructure is characterised by neck formation between the zircon particles. The smaller grains exhibit rounded surfaces whereas the large particles still possess the blocky shape of the original grits. No phase separation is observed (Fig. 11). After 5 h at 1600 °C the first evidence of ZrO_2 is recognized both by XRD and SEM. ZrO_2 starts to nucleate at grain boundaries and particle surfaces of zircon. The ZrO_2 particles are enveloped by a thin layer of amorphous silica. At 1650 °C the amount of ZrO_2 increased significantly whereas the residual zircon particles get smaller and progressively rounded (Fig. 12). Between the zirconia particles a new kind of liquid phase is clearly distinguished from the amorphous SiO_2, consisting of 62.6 wt.% SiO_2, 27.1 wt.% ZrO_2, and 10.3 wt.% Al_2O_3 coming from the impurities.

After 5 h at 1700 °C (Fig. 13), the amount of dendritic ZrO_2 precipitates has grown. Most of the aggregates are located at surfaces of residual zircon crystals but some are also generated inside. Obviously, the decomposition of zircon starts at particle surfaces or two-dimensional crystal imperfections releasing columnar ZrO_2 particles separated by amorphous SiO_2. Changes in specific volume ($ZrSiO_4$ (0.22 cm^3/g or 40.33 cm^3/mol) = SiO_2 (0.46 cm^3/g or 27.64 cm^3/mol) + ZrO_2

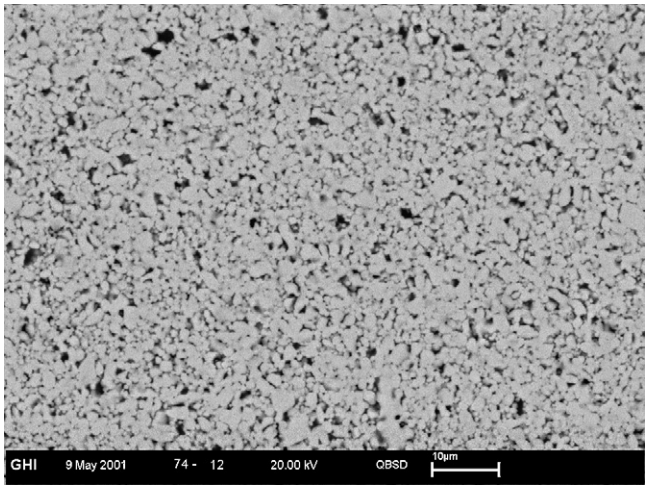

Fig. 9. $ZrSiO_4 < 1\ \mu m$, 4 h anneal at 1500 °C, black: glassy phase and pores, grey: $ZrSiO_4$. Scale = 10 μm.

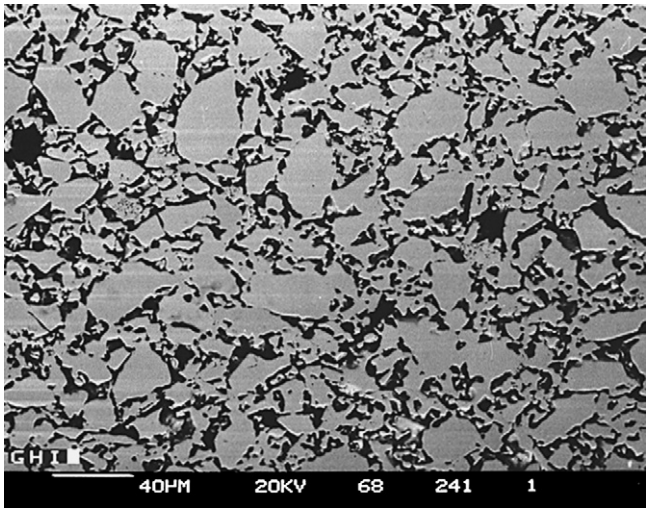

Fig. 11. Calcined zircon (powder E) sintered 5 h at 1500 °C. Scale = 40 μm.

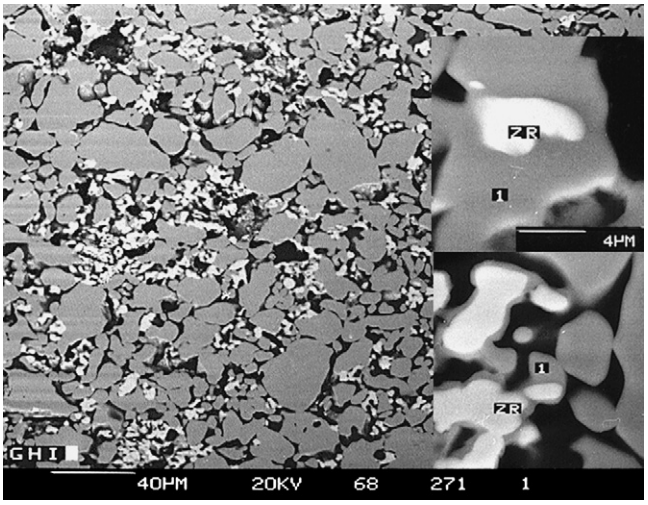

Fig. 12. Calcined zircon (powder E) sintered 5 h at 1650 °C. Scale = 40 μm. ZR = ZrO_2; [1] = $ZrSiO_4$; (right) close-ups of the larger figure.

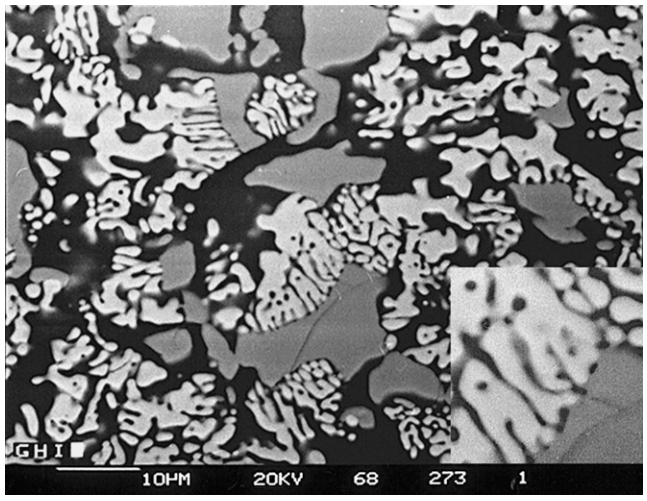

Fig. 14. Close-ups of Fig. 13. Note dark grey SiO_2 between the white ZrO_2-dendrites, large grey particles: residual $ZrSiO_4$, black: AZS-liquid phase. Scale = 10 μm.

(0.17 cm^3/g or 20.95 cm^3/mol)) give rise to the formation of small pores inside the dendrites (Fig. 14) or at the interface between zircon and zirconia. A closer look at the dendrites reveals that they all are covered by a thin rim of amorphous silica which separates these aggregates from an increasing volume of a AZS-liquid phase now containing 81.1 wt.% SiO_2, 13.5 wt.% ZrO_2, and 5.4 wt.% Al_2O_3.

The XRD analysis of all $ZrSiO_4$-based samples did not show any significant differences. It should be noted, however, that the sintered samples were furnace cooled and not quenched so that some retrograde reactions yielding zircon formation (see Table 3) must be taken into account. $ZrSiO_4$ is the only present phase in the sintered samples at temperatures below 1500 °C. Powders of 98% purity start to decompose under formation of ZrO_2 between 1500 and 1550 °C depending on the initial grain size. The ZrO_2-content increases slowly up to 1650 °C, and faster at higher temperature, as can be seen from the X-ray diagrams in Fig. 15. The decomposition temperature determined under these conditions is thus located between 1500 and 1550 °C. In materials with 100% purity, the formation of ZrO_2 can only occur at a temperature above 1600 °C although the very small grain size is expected to provide a high driving force and excellent nucleation conditions for the decomposition. Consequently, it must be stated that impure material tends to decompose at lower temperature than the pure compound. The modifications of zirconia found after cooling were both tetragonal and monoclinic, depending on the grain size of the particles formed at high temperature.

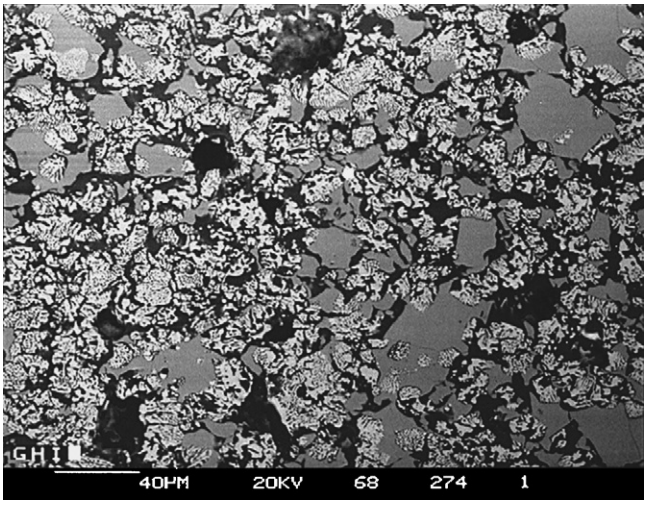

Fig. 13. Calcined zircon (powder E) sintered 5 h at 1700 °C. White: ZrO_2, grey: residual $ZrSiO_4$, black: AZS-liquid phase. Scale = 40 μm.

4.3. Sintering of ZrO_2–SiO_2 mixes

At 1200 °C and after 2 h anneal all samples exhibit the starting compounds only but the submicron ZrO_2 particles have grown to re-crystallised aggregates of 0.5–1 μm in diameter. After 4 h, however, small crystallites of $ZrSiO_4$ are formed between ZrO_2 particles. After 5 h at 1500 °C a large amount of both unstabilised and Y-stabilised ZrO_2 particles transformed to $ZrSiO_4$ (Fig. 16).

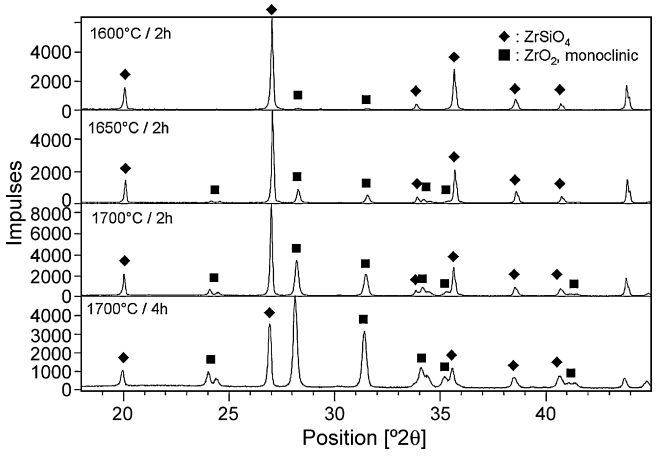

Fig. 15. XRD spectra of $ZrSiO_4$, grain size <9 μm, annealed at various temperatures.

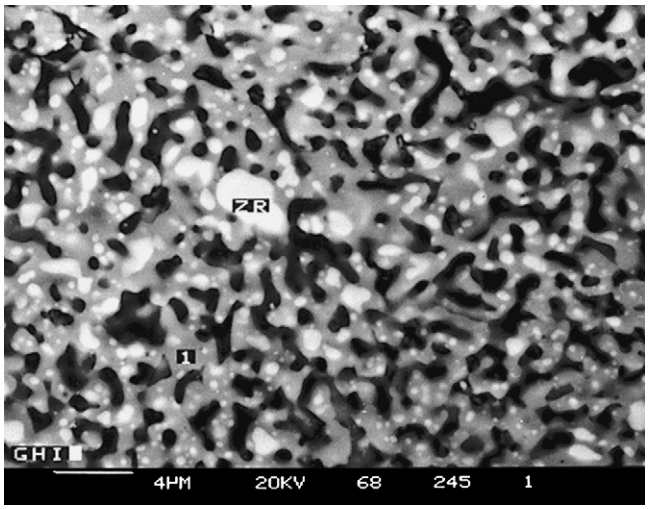

Fig. 16. Aerosil 200/fumed ZR-TZ, 5 h anneal at 1500 °C; light grey: $ZrSiO_4$, white: ZrO_2, dark grey, black: SiO_2. Scale = 4 μm.

The zirconia particles are entirely embedded in newly formed zircon aggregates with interconnecting sinter necks creating a spongy structure. Residual amorphous silica is located between the branches of zircon. This implies that zircon is formed by a diffusion reaction at the ZrO_2–SiO_2 interface until ZrO_2 was almost entirely consumed (Fig. 17). At higher temperatures, i.e. at 1700 °C, the amount of zircon decreases again. After 2 h the microstructure contains very fine-grained ZrO_2 embedded in residual zircon and amorphous silica (Fig. 18). Prolonged annealing for 5 h results in clusters of rounded ZrO_2 slightly grown to 1–2 μm and surrounded by a thin skin of residual zircon (Fig. 19). The space between the ZrO_2/$ZrSiO_4$ areas is filled by amorphous silica. This reminds to the microstructures obtained in the initial state of zircon decomposition shown in Fig. 12 where isolated ZrO_2 is also enveloped in a thin layer of $ZrSiO_4$.

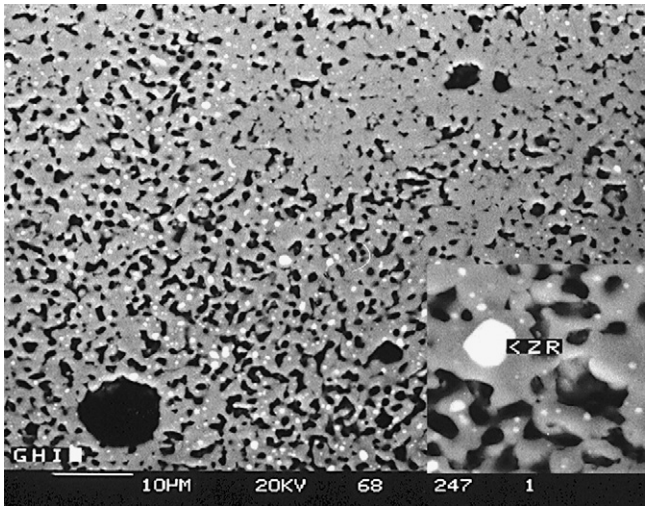

Fig. 17. Aerosil 200/fumed ZR-TZ, 5 h anneal at 1600 °C; light grey: $ZrSiO_4$, white: residual ZrO_2, black: pores and residual SiO_2, close-up at the lower right corner. Scale = 10 μm.

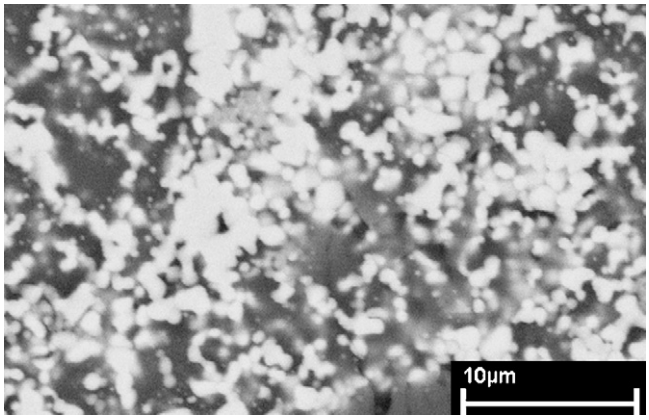

Fig. 18. Aerosil 200/TZ-3Y, 2 h at 1700 °C; light grey: $ZrSiO_4$, white: ZrO_2, dark grey, black: SiO_2.

XRD characterisation of sintered samples reveals that in case of ZrO_2/SiO_2 mixes the temperature of zircon formation depends strongly on the kind of ZrO_2 powders used. Thus, unstabilised zirconia reacts to form zircon already at 1200 °C after 4 h. In case of yttria-stabilised ZrO_2 no zircon can be found by XRD even after 6 h at 1200 °C. The formation of zircon was observed from 1300 °C upwards. In all cases the maximum content of zircon is obtained at 1500 °C, approximately. At higher temperatures, the ZrO_2-content increases again. In contrast to these results, almost no notable dependence of the zircon formation start-temperature on the type of silica (fused and fumed silica, as well as cristobalite of different grain size) used for the mixtures with zirconia was observed. Cristobalite is formed, however, in case of both Aerosil 200 and fused silica as starting compounds after 2 h at 1400 °C and, in case of thermally decomposed zircon, already after 4 h at 1200 °C. Once formed, cristobalite proved to be very stable. Cristobalite reacted completely with zirconia only in the case of thermally decomposed zircon above 1400 °C after 4 h and, in case of ultra fine grain size, at 1700 °C.

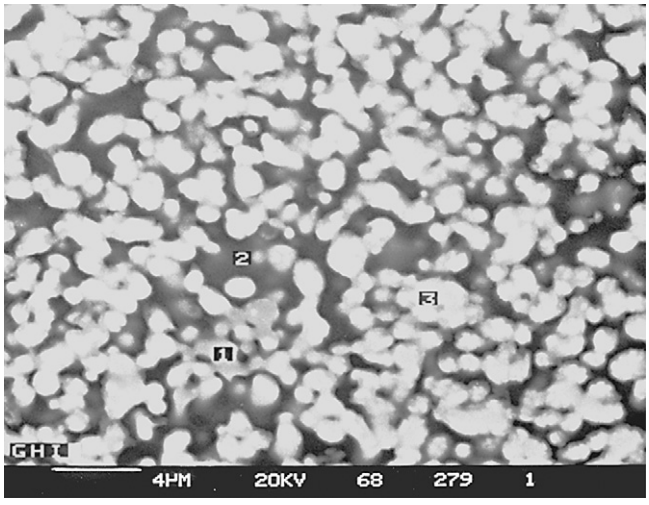

Fig. 19. Aerosil 200/fumed ZR-TZ, annealed 5 h at 1700 °C; [1], residual $ZrSiO_4$; [2], SiO_2; [3], ZrO_2. Scale = 4 μm.

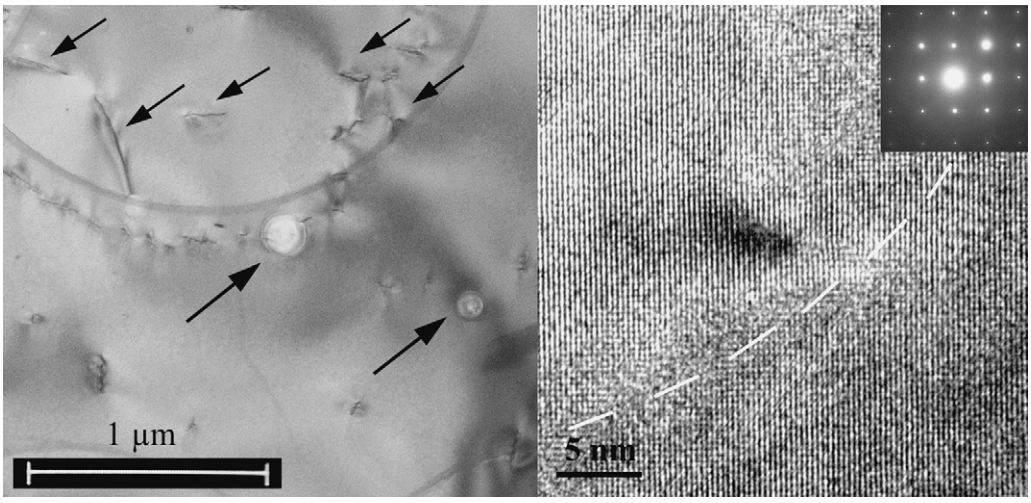

Fig. 20. (Left) TEM micrograph of single crystal annealed at 1650 °C, 16 h; uphill arrows point to spherical segregation areas, downhill arrows indicate dislocations. (Right) HR-TEM figure of border zone between segregation area (top of dashed white line) and unaffected crystal (below). Note that there is no indication of phase changes or any major lattice deformation.

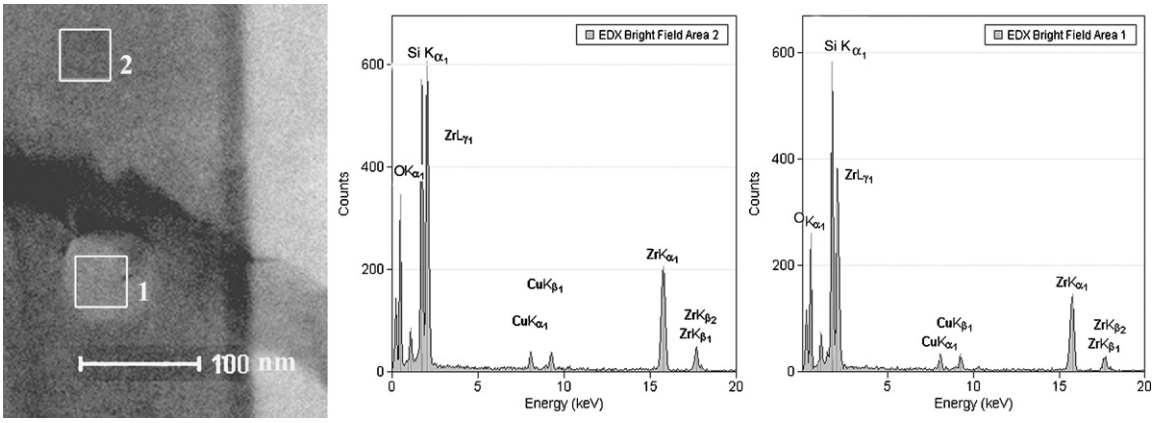

Fig. 21. STEM-analysis from light spherical areas (1) and unaffected area (2) of a zircon single crystal annealed at 1650 °C for 16 h and water quenched.

4.4. Zircon single crystal studies on decomposition temperature

The experiments using slices of a zircon single crystal were carried out in the temperature range between 1650 and 1700 °C. In the water-quenched 1650 °C samples (4–16 h holding time) no ZrO_2 was observed by both SEM and HR-TEM. Instead, the samples show the formation of spherical areas of up to 100 nm in diameter that contain a SiO_2-rich phase, as determined by EDS-analysis, which will be subject for further characterisation work. Fig. 20 presents TEM micrographs of a single crystal slice annealed at 1650 °C for 16 h. It is obvious that spherical areas of lighter contrast were generated inside the crystal by homogeneous nucleation which, however, does not yield any evidence for the formation of a second phase. In spite, comparative STEM-measurements of these areas and the unaffected environment confirm that the silicon content inside the spheres is significantly higher than in ordinary zircon (Fig. 21).

After heating to 1660 °C, i.e. only 10 K higher than the sample presented before (no isothermal hold as well), many zirconia particles have formed at the surface of the crystal by heterogeneous

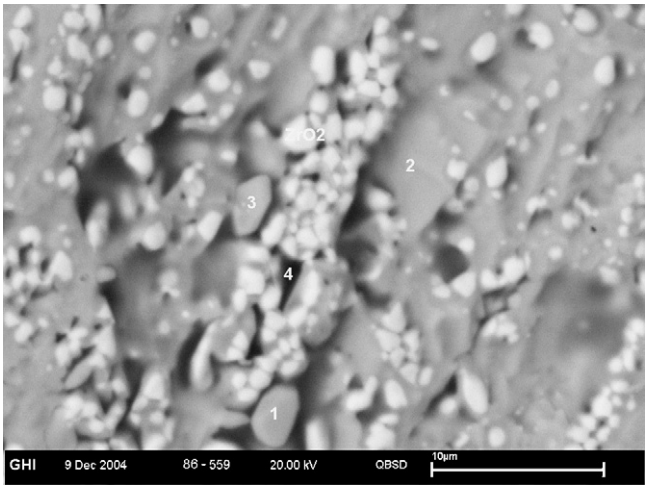

Fig. 22. Single crystal annealed at 1660 °C, no holding time. Scale = 10 µm.

Table 4
Semi-quantitative EDS-analysis of single crystal surfaces after heating to 1660 °C without isothermal annealing, numbers refer to Fig. 22

	No. 1 Zircon	No. 3 Zircon	No. 2 SiO_2-depleted area	No. 4 SiO_2-enriched area
SiO_2 (mol%)	49.2	50.5	47.3	66.3
ZrO_2 (mol%)	50.8	49.5	52.7	33.7

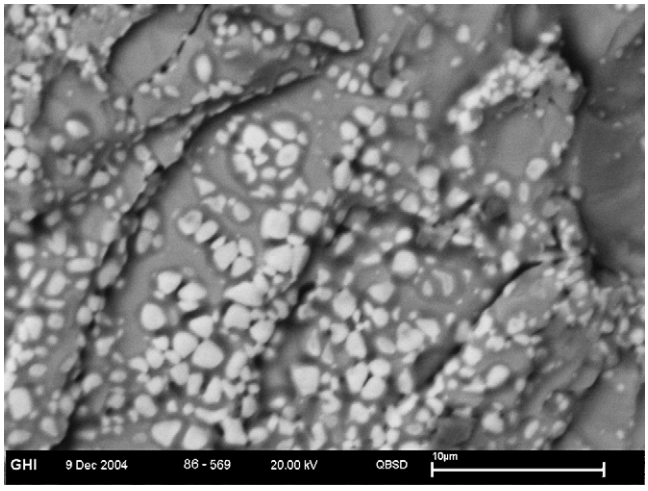

Fig. 23. Surface of a zircon single crystal slice as heated to 1680 °C; white: ZrO_2, for composition of the numbered areas refer to text. Scale = 2 μm.

nucleation being surrounded by areas of different atomic number contrast (Fig. 22). The EDX analysis is given in Table 4 and may be interpreted as the stoichiometry of a hypothetic $ZrSi_2O_6$ compound (point 4 in Fig. 22). Possibly these areas act as nucleation site for stable or metastable decomposition products of $ZrSiO_4$. Of course, due to the small area measured these analyses have to be taken as semi-quantitative, and, hence, more TEM-studies are required to prove the results.

The SEM micrograph of the sample annealed at 1680 °C, no holding time, shows the continuous formation of ZrO_2 precipitates (white phases in Fig. 23) surrounded by various areas of changing SiO_2-content (see Fig. 24). Point No. 4 in Fig. 24 is $ZrSiO_4$ with a molar SiO_2-to-ZrO_2 ratio of 1.0, whereas this ratio

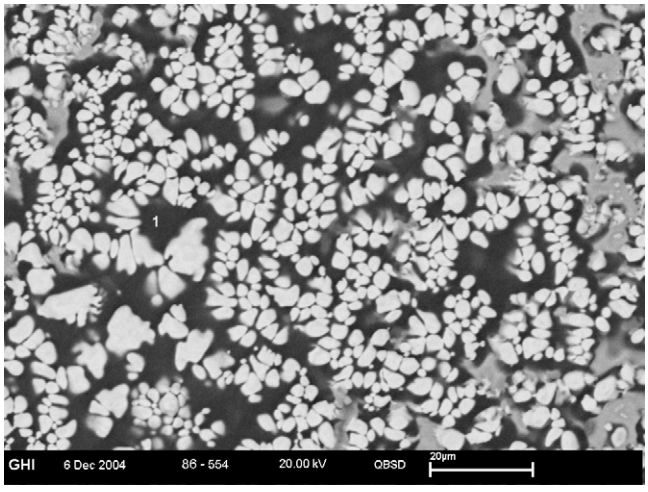

Fig. 24. Surface of a zircon single crystal slice as heated to 1680 °C; white: ZrO_2, for composition of the numbered areas refer to text. Scale = 2 μm.

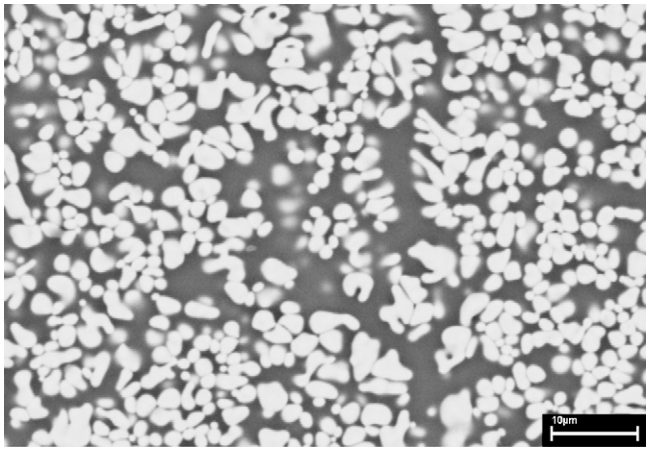

Fig. 25. Liquid phase formation in single crystals heated to 1700 °C, 1h annealing time. Scale = 10 μm.

is 0.74 at point 3, 1.15 at point 2, and 1.49 at point 1 indicating an increase in SiO_2 by this order.

Above 1680 °C the formation of a liquid phase was observed in the single crystal samples. Here, a growth of dendritic ZrO_2 is initiated which is oriented almost perpendicular to the $ZrSiO_4$-surface with a presumably amorphous silica phase in between. After 1 h at 1700 °C a eutectic microstructure develops (Fig. 25) with ZrO_2 (white) and an amorphous silicon-oxide containing at about 3 at.% zirconium.

5. Discussion

5.1. Zircon decomposition in powder-based materials

This study reveals that commercial zircon-based products of "100%" purity start to decompose at 1600 °C and no soaking time under formation of zirconia and an amorphous SiO_2 phase. The velocity of decomposition accelerates significantly at temperatures above 1650 °C. The ZrO_2 formed is usually tetragonal phase in agreement with its thermodynamic stability range. Large particles, i.e. >2–5 μm, may, however, transform spontaneously to monoclinic during cooling and thus cause some confusion when detected by X-ray diffraction at room temperature.

Both purity and grain size influence strongly the temperature and rate of zircon decomposition. According to HT-XRD, the reaction starts between 1450 °C (98% $ZrSiO_4$, <3 μm) and 1600 °C (100% $ZrSiO_4$, <1 and <4 μm, respectively).

Generally, two temperature ranges of the reaction have been recognized in the literature given their different decomposition velocities (Figs. 3 and 4). Our experiments yield also evidence that the decomposition is rather slow at temperatures below 1650 °C and faster at higher temperatures. Thus, both literature results[11,12] can be re-interpreted quantitatively. First of all, both

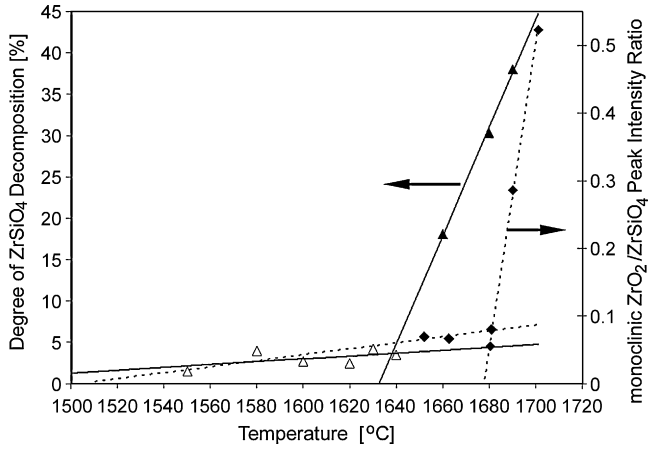

Fig. 26. Degree of zircon composition, a re-interpretation of Anseau et al. (triangles and full line[11]) and Klute (quadrangles and dotted line[12]).

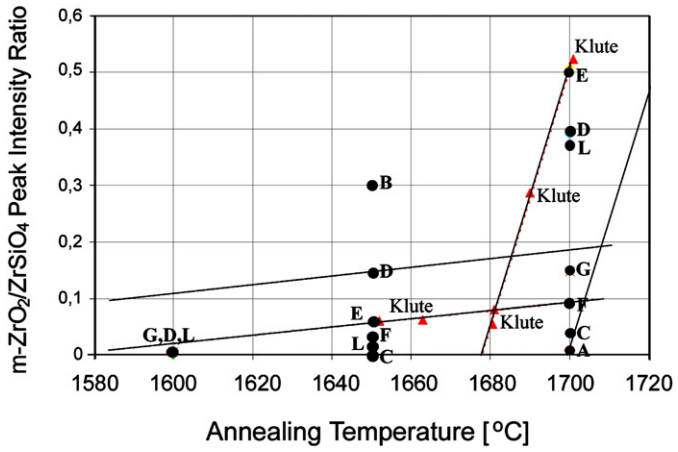

Fig. 27. Degree of zircon decomposition after 2 h annealing time.

figures give kinetic rather than equilibrium information for the decomposition. The original diagram of Anseau et al.[11] shows one continuous curve of increasing slope. Another interpretation is possible, however, which is that there are two reaction mechanisms, each being represented by one straight line. The point of line intersection thus means a change in reaction kinetics whereas the extrapolation of the line with the steep slope to 0% decomposition gives the onset of a thermally induced decomposition. In Fig. 26 the original data in Figs. 3 and 4 are re-drawn and approximated by two linear regressions, the slope being a function of activation energy.

As mentioned earlier, the temperatures of intersection are 1630 and 1681 ± 5 °C, Anseau and Klute, respectively, the temperatures of 0% decomposition at fast rate are 1622 and 1676 °C, respectively. Similarly, the extrapolated onsets of the dissociation at slow rate are 1425 and 1503 °C (extrapolated through three points only), respectively.

Now, the difference between the two results is the purity of the starting material, 99.28% (impurities 0.32 wt.% Al_2O_3, 0.25 wt.% TiO_2, 0.15 wt.% Fe_2O_3) in case of Anseau's material, 100% in the latter case. The comparison implies that impurities may shift the dissociation onset to lower temperatures, which is also confirmed by our results obtained with powders of less purity.

The data obtained in the present work fit very well into Fig. 26. Samples annealed for 2 h at the particular temperature show a slightly lower degree of transformation when compared to Klute's data obtained after annealing for 1–2 days, which is readily expected. Fig. 27 gives a summary of the results as measured from the *m*-$ZrO_2/ZrSiO_4$ XRD peak intensity ratio. The lines indicate the upper bounds of the transformation areas as well as the transformation functions from Fig. 26. Additionally Fig. 27 shows the grain size dependence of the zircon decomposition as powders B, D and F are the same raw material but with different grain sizes. With decreasing grain size and increasing specific surface area (F → D → B) an increased dissociation rate of zircon is observed. For powders E and F, which have the same specific surface area and comparable grain sizes, powder E with the lower purity grade shows the higher dissociation rate, especially at 1700 °C, where already a large amount of liquid phase has formed.

5.2. Formation of zircon from oxide blends

The formation of zircon from mixed oxides starts at 1200 °C, depending on whether the initial zirconia was stabilised by dopands or not. The maximum formation rate was observed between 1500 and 1550 °C in all cases, at higher temperatures the $ZrSiO_4$-concentration decreases again. Amorphous SiO_2 tends to crystallise as cristobalite prior to the reaction, and the use of unstabilised zirconia results in the monoclinic-to-tetragonal transformation between 1170 and 1200 °C as proved by HT-XRD and DTA. Since zircon nucleates at the interface between ZrO_2 and SiO_2, the reaction seems to be diffusion controlled. This means that the zircon interlayer broadens by diffusion either of silicon or of zirconium through the layer to the opposite side. Since the Si^{4+} ion is significantly smaller than the Zr^{4+} ion and the latter is already arranged in ZrO_8 polyhedra which have only to separate in one direction in order to incorporate SiO_2, the preferred diffusion of silicon as $[SiO_5]^{6-}$ is most likely. Furthermore, it is obvious that in the presence of cristobalite, either coming from the raw materials or being generated by the crystallisation of amorphous silica, the reaction rate is much slower because cristobalite is still observed after 4 h at 1500 °C. At higher temperatures the reverse process is initiated: zirconia is nucleated heterogeneously at the grain boundaries of zircon. In this case the release of silica is easier since the higher temperature allows the expansion of the ZrO_8-coordination in the tetragonal ZrO_2 structure without elastic stresses whereas SiO_2 may be dissolved already in the liquid if impurities are present.

5.3. Single crystal experiments

The single crystal results indicate that the decomposition of the $ZrSiO_4$ starts as a solid-state reaction through the formation of different metastable intermediate phases with increasing Si-content in form of a gradual enrichment in SiO_2. Because of the smaller ionic radius of Si^{+4} (0.26 Å) the silicon shows higher diffusion velocities compared to the larger Zr^{+4} (0.72 Å) which

prefers to maintain its eightfold coordination from the $ZrSiO_4$-structure in the tetragonal ZrO_2-structure, which is the stable ZrO_2 modification in the temperature range under consideration (1650–1700 °C). As a consequence, the ZrO_8-coordination polyhedra in the $ZrSiO_4$-structure which are interconnected by SiO_4-tetraedra along the *c*-axis become separated by the outward diffusion of the Si^{+4} (as $[SiO_5]^{-6}$) while they start forming zirconia-units in *b*-direction. As interpreted before, the ZrO_8-units try to expand with increasing temperature and are thus under compressive stresses if there are still SiO_4-tetrahedra in the chain. Accordingly, the release of SiO_2 results in a relaxation of the structure, and ZrO_2 is formed upon rearrangement.

Special attention for further investigations has to be paid to one of the observed metastable intermediate phases formed at 1660 and 1680 °C that exhibits an ideal 66 at.% SiO_2 and 33 at.% ZrO_2 compositions corresponding to a virtual "$ZrSi_2O_6$" compound. $ZrSi_2O_6$ is not a stable phase in the ZrO_2–SiO_2 phase diagram but possibly corresponds to the $ZrTi_2O_6$-phase in the ZrO_2–TiO_2 system.[15] Similar to $ZrSiO_4$, the $ZrTi_2O_6$-phase, also known as srilankite, decomposes peritectically forming a disordered $(Zr, Ti)_2O_4$ having a unit cell very similar to that of tetragonal Ti-stabilised zirconia.[16] Most probably it is because of this intermediate metastable compound that cristobalite is not found even during solid-state decomposition of zircon single crystals.

The results of the single-crystal experiments agree with the dissociation temperatures of $ZrSiO_4$ into ZrO_2 and SiO_2 as given by Butterman and Foster,[4] Jones et al.,[17] and Klute.[12] These references agree also reasonably in respect to the eutectic temperature (liquid ↔ tetragonal ZrO_2 + β-cristobalite) and have therefore been taken into account for further data assessment.

5.4. Thermodynamic considerations

Using the data mentioned above[4,12,17] and from present work, the thermodynamic ZrO_2–SiO_2 dataset in FACTSage[18] was optimized. In FACTSage the heat capacity and standard entropy of formation for $ZrSiO_4$ were taken from.[19] The standard enthalpy of formation given by[19] (−2,023,801 J/mol) was corrected in FACTSage to obtain a dissociation temperature for $ZrSiO_4$ of 1538 °C as published by,[5] also taking the experimental results of[11] into consideration.

Since most of the previously described experiments reveal uncertainties the data of Butterman et al.,[4] Jones et al.[17] and Klute[12] were used in the present work as most reliable, settling the dissociation temperature of $ZrSiO_4$ at 1676, 1675 ± 10 and 1681 ± 5 °C, respectively. The enthalpy of formation published by Barin[19] was adjusted resulting in a dissociation temperature of 1673 °C, which is in good agreement with the experimental values of Ellison and Navrotzky[20] and those given in the thermodynamic databases of Knacke et al.[21] and Kubaschewski and Alcock.[22]

For the calculation of the liquid phase, the quasi-chemical-model in FACTSage was used yielding a eutectic temperature of 1687 °C, in agreement with the experimental values of 1685 ± 10,[17] 1687 ± 4,[4] and 1699 ± 3 °C.[12] The phase diagram calculated accordingly is shown in Fig. 28. Here the immiscibility gaps considered by Curtis and Sowman[5] and Butterman Foster[4] were taken into account although the origin of these data is uncertain and not proved.

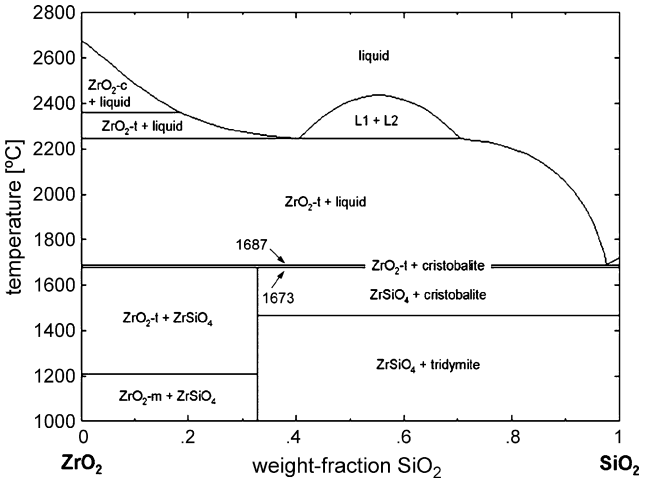

Fig. 28. Optimised calculated ZrO_2–SiO_2 phase diagram.

As the temperature difference between the decomposition of $ZrSiO_4$ by a solid-state reaction and the formation of the first liquid is only 14 K, it is evident that even minor impurities in the zircon raw material lead to a decrease of the eutectic temperature below the dissociation temperature. As a consequence, the solid-state dissociation in most cases is superimposed by the formation of a lower melting silicate liquid in which the natural impurities are concentrated. From solid zircon essentially SiO_2 is released and subsequently dissolved in the liquid phase leaving solid ZrO_2 behind. This fact might explain the contradictory statements in literature concerning both the decomposition mechanism and temperature. The newly developed thermochemical dataset of the ZrO_2–SiO_2 system in combination with the FACTSage[18] databases enables calculations in the ZrO_2–SiO_2–FeO–Fe_2O_3–TiO_2–Ti_2O_3–MgO and higher order systems containing the main impurities of natural zircon raw materials and therefore will be used to examine the influence of certain impurities in zircon raw materials on the $ZrSiO_4$ decomposition.

Thus the impurities of the raw materials given in literature for example by Anseau et al.[11] can be considered in thermochemical calculations. Therefore, a composition of 99.28 wt.% $ZrSiO_4$, 0.32 wt.% Al_2O_3, 0.25 wt.% TiO_2, and 0.15 wt.% Fe_2O_3 was calculated yielding evidence for the first formation of a liquid phase at 1227 °C. The existence of a liquid phase allows the dissolution of silica as soon as it is released from the zircon crystal as a solid (crystalline or amorphous) phase. Applying the data set by Wu[23] an impurity-derived liquid phase is formed at 1538 °C and therefore present throughout all temperatures used in the experiments by Anseau et al.[11] Calculation of the phase reactions of the isolated impurities, i.e. without zircon, reveals a melting point of as low as 1302 °C. Similar results are obtained by Shi et al.[24] who synthesised zircon from zirconium oxychloride sol and Aerosil by hot pressing and found a small amount of liquid phase at the grain boundaries consisting of 0.11 wt.% Al_2O_3 and 0.029 wt.% Fe_2O_3.

6. Conclusion

The liquid phase due to natural or processing-inherent impurities obviously controls the kinetics of zircon decomposition. Thus more or less all experimental data suffer from the problem that the peritectoidal dissociation of zircon is superimposed by the kinetic of liquid phase-driven dissolution of the solid silica generated as dissociation product. Since the amount of liquid phase increases with temperature, the decomposition rate accelerates with temperature and time, too. Thus the first reaction, exhibiting a small slope in the decomposition rate, may be attributed to solid-state diffusion/dissolution-controlled reactions, whereas the decomposition reaction with a steep slope indicates that the eutectic temperature between zirconia and cristobalite was also lowered by impurities of the raw materials. Thus even the results of "100%" pure materials should be re-investigated with more accuracy since some impurities (<0.01%) were possibly also present.

The significant influence of even very small amounts of impurities explains also the grain size sensitivity of the decomposition temperature: as a larger surface area is created, lattice defects are generated and diffusions distances are lowered—facts enabling fast nucleation, an easy release of silica, and providing an excellent contact with liquid impurities. This is in particular important for natural zircon because these crystals usually contain very small inclusions of rutile, magnetite, garnet, spinels, xenotime, monazite, apatite, and others giving raise to local melting. Furthermore, it should be noted that zircon hosts both Hf^{4+} and Th^{4+} in solid solution which may also lower the decomposition temperature. It is, however, proved by the experiments that the grain size effect is exceeded by far by the influence of impurities.

In almost all cases reported and measured in our experiments, the resulting liquid phase approaches the concentration of the ternary eutectic as reported by Greca et al.[25] In the alumina-rich corner of the Al_2O_3–SiO_2–ZrO_2 system, leaving the question open if mullite is melting congruently or incongruently, a ternary eutectic appears at 1550 °C which may give rise to the lower decomposition point of zircon. It should be noted that in the alumina-rich corner also a small stability field of zircon plus liquid is existing.

In general, the phase diagrams of all higher systems including ZrO_2–SiO_2 subsystems should be revised.

In case of pure single crystals it is worth while noting that the release of SiO_2 in the solid state occurs along certain crystallographic planes by local accumulation of SiO_2 with ZrO_2 neighbourhood. The formation of an intermediate metastable zirconium silicate $ZrSi_2O_6$ is most likely, but needs further experimental proof. This fact may be considered the reason why the cristobalite formation is suppressed and a liquid phase formation is favoured instead at slightly higher temperatures.

Acknowledgement

This study was kindly supported by the German Research Foundation (Deutsche Forschungsgemeinschaft) under the grant No. Te 146/14-1,2 which is gratefully acknowledged.

References

1. Boggum, P., Schulte, K. and Glaser, W., Sicherheit im Boden von Glasschmelzwannen. *Sprechsaal*, 1983, **116**(5), 386–392.
2. Schulle, W., *Feuerfeste Werkstoffe-Feuerfestkeramik-Eigenschaften, prüftechnische Beurteilung, Werkstofftypen, Feuerfeste Werkstoffe*, 1st ed., Deutscher Verlag für Grundsoffindustrie, Leipzig, Germany, 1990.
3. Washburn, E. W. and Libman, E. E., Approximate determination of melting point diagram of zirconia–silica. *J. Am. Ceram. Soc.*, 1920, **3**, 634–640.
4. Butterman, W. C. and Foster, W. R., Zircon stability and the ZrO_2–SiO_2 phase diagram. *Am. Mineral.*, 1967, **52**, 880–885.
5. Curtis, C. E. and Sowman, H. G., Investigation of the thermal dissociation, reassociation, and synthesis of zircon. *J. Am. Ceram. Soc.*, 1953, **36**(6), 190–195.
6. Toropov, N. A. and Galakhov, F. Yu., Liquidation in the system ZrO_2–SiO_2. *Izv. Akad. Nauk. USSR, Ser. Khim.*, 1956, **2**, 158–161.
7. McPherson, R., Rao, R. and Shafer, B. V., The reassociation of plasma dissociated zircon. *J. Mater. Sci.*, 1985, **20**, S.2597–S.2602.
8. Mori, T., Yamamura, H., Kobayashi, H. and Mitamura, T., Formation mechanism of $ZrSiO_4$ powders. *J. Mater. Sci.*, 1993, **28**, 4970–4973.
9. Kanno, Y., Thermodynamic and crystallographic discussion of the formation and dissociation of zircon. *J. Mater. Sci*, 1989, **24**, 2415–2420.
10. Tartaj, P., Serna, C. J., Moya, J. S., Requena, J., Ocana, M., De Aza, S. and Guitian, F., The formation of zircon from amorphous $ZrO_2{\cdot}SiO_2$ powders. *J. Mater. Sci.*, 1969, **31**, 6089–6094.
11. Anseau, M. R., Biloque, J. P. and Fierens, P., Some studies on the thermal stability of zircon. *J. Mater. Sci.*, 1976, **11**(3), 578–582.
12. Klute, R., *Phasenbeziehungen im System Al_2O_3–Cr_2O_3–ZrO_2–SiO_2 unter besonderer Berücksichtigung des korundhaltigen Bereiches,* Diplomarbeit RWTH Aachen Germany, Lehrstuhl für Technische Mineralogie (Chair of Applied Mineralogy), Supervisor: Woermann, E., 1982.
13. Reijnen, P., Bastius, H., Faizullah, M. and Kamtz, H., Nasschemische Methoden zur Erzeugung von synthetischen Rohstoffen und von homogenen Pulvern für physikalisch-chemische Untersuchungen. *Ber. Dt. Keram. Ges.*, 1977, **54**, 63–68.
14. Pavlik, R. S., Holland, H. J. and Payzant, E. A., Thermal decomposition of zircon refractories. *J. Am. Ceram. Soc.*, 2001, **84**(12), 2930–2936.
15. Troitzsch, U. and Ellis, D. J., High-pT-studies of solid solutions in the system ZrO_2–TiO_2: the stability of srilankite. *Eur. J. Mineral.*, 2004, **16**, 577–584.
16. Newnham, R. E., Crystal structure of $ZrTiO_4$. *J. Am. Ceram. Soc.*, 1967, **50**, 216.
17. Jones, T. S., Kimura, S. and Muan, A., Phase relations in the system FeO–Fe_2O_3–ZrO_2–SiO_2. *J. Am. Ceram. Soc.*, 1967, **50**, 137–142.
18. Bale, C. W., Chartrand, P., Degterov, S. A., Eriksson, G., Hack, H., Ben Mahfoud, R., Melançon, J., Pelton, A. D. and Petersen, S., FactSage thermochemical software and databases. *Calphad: Comput. Coupling Phase Diagrams Thermochem.*, 2002, **26**(2), 189–228.
19. Barin, I., *Thermochemical Data of Pure Substances*, *vols. 1 and 2*. VCH Verlagsgesellschaft, Weinheim, 1989.
20. Ellison, A. J. G. and Navrotzky, A., Enthalpy of formation of zircon. *J. Am. Ceram. Soc.*, 1992, **75**, 1430–1433.
21. Knacke, O., Kubaschewski, O., Hesselmann, K., *Thermochemical Properties of Inorganic Substances, Vols. I and II*, Springer-Verlag Berlin, Heidelberg, Verlag Stahleisen mbH, Düsseldorf, 1991.
22. Kubaschewski, O. and Alcock, C. B., *Metallurgical Thermochemistry* (*5th ed.*). Pergamon Press, London, 1979.
23. Wu, P., *Optimisation and Calculation of Thermodynamic Properties and Phase Diagrams in Multi-Component Oxide Systems, PhD Thesis*, University of Montreal, 1992.
24. Shi, Y., Huang, X. and Yan, D., Effect of natural zircon powder as seeds on the gel synthesis of zircon powder. *Mater. Lett.*, 1994, **21**, 79–83.
25. Greca, M. C., Emiliano, J. V. and Segadaes, A. M., Revised phase equilibrium relationships in the system Al_2O_3–ZrO_2–SiO_2. *J. Eur. Ceram. Soc.*, 1992, **9**, 271–283.